



An acidless microwave-assisted wet digestion of biological samples as a greener alternative: applications from COVID-19 monitoring to plant nanobiotechnology

Ana Beatriz Santos da Silva^{1,2,3} · Ketolly Natanne da Silva Leal^{1,2} · Marco Aurélio Zezzi Arruda^{1,2}

Received: 28 May 2024 / Revised: 12 July 2024 / Accepted: 24 July 2024

© The Author(s), under exclusive licence to Springer-Verlag GmbH, DE part of Springer Nature 2024

Abstract

Sample preparation in an analytical sequence increases the number of errors, is highly time-consuming, and involves the manipulation of hazardous reagents. Therefore, when an improvement in an analytical method is required, the sample preparation step needs to be optimised or redesigned. Moreover, this step can involve significant toxic reagents and a high volume of waste. In that regard, this study proposes a new procedure based on microwave-assisted wet digestion combining two green strategies: a miniaturised system (with a few microlitres of volume) and the only use of hydrogen peroxide. Three biological samples (human serum, urine, and plant in vitro material) were chosen due to their high potential for disease monitoring, toxicological studies, and biotechnology applications. Several trace elements (Ca, Cd, Co, Cu, Fe, Mg, Mn, Mo, Ni, Se, and Zn) were determined by inductively coupled plasma optical emission spectroscopy and inductively coupled plasma mass spectrometry. For human serum and urine, a certified reference material was used to check for accuracy; the recovery ranged from 72% (Cd, ICP-MS) to 105% (Mg, ICP OES) for serum, while for urine, they varied from 82% (Ni, ICP-MS) to 122% (Zn, ICP-MS). For the soybean callus sample (in vitro plant material), a comparison between the proposed method and the acid digestion method was conducted to evaluate the accuracy, and the results agreed. The detection limits were 0.001–60 $\mu\text{g L}^{-1}$ (lowest for Cd), thus demonstrating a suitable sensitivity. Moreover, the decomposition efficiency was demonstrated by determining the residual carbon, and a low amount was found in the final product digested (below 0.8% w v⁻¹). A green metric approach was calculated for the proposed method, and according to AGREEprep software, it was found to be around 0.4. Finally, the method was applied to urine samples collected in patients with COVID-19 and soybean callus cultivated with silver nanoparticles. This sample preparation method is a new acidless and miniaturised alternative for elemental analysis involving biological samples.

Keywords Hydrogen peroxide · In loco acid generation · Green method · Sample preparation · Biological samples

Published in the topical collection featuring *Sustainability in Sample Preparation* with guest editors Soledad Cárdenas and Pablo Richter.

✉ Marco Aurélio Zezzi Arruda
zezzi@unicamp.br

¹ Spectrometry, Sample Preparation and Mechanization Group, Institute of Chemistry, University of Campinas – Unicamp, P.O. Box 6154, Campinas, SP 13083-970, Brazil

² National Institute of Science and Technology for Bioanalytics, Institute of Chemistry, University of Campinas – Unicamp, P.O. Box 6154, Campinas, SP 13083-970, Brazil

³ Present Address: Center of Environmental Studies, São Paulo State University, Rio Claro 13506900, Brazil

Introduction

Although green analytical chemistry (GAC) recommends direct analysis, many techniques, including plasma-based techniques such as inductively coupled plasma optical emission spectroscopy and inductively coupled plasma mass spectrometry, demand converting a solid sample into a liquid. Considering this kind of analysis, the sample preparation procedure is unquestionably the most critical and influential step in achieving suitable conditions for GAC [1, 2]. Moreover, it is well established that this step is both a major source of error and time-consuming [3]. As sample preparation cannot be neglected and was not previously incorporated into GAC principles, a recent work proposed that the 10 green sample preparation (GSP) principles are

interconnected. To overview, these principles recommend safer methodologies for the analyst, minimise both energy and reagent volumes or amounts, and employ automation and miniaturisation [4, 5].

When elemental analysis is performed on biological samples (e.g. serum, blood, cerebrospinal fluid, urine, biomolecules, and cells), acid digestion, mainly with nitric acid, is commonly reported [2, 6]. On the other hand, new methodologies have been proposed to reduce the amount of samples used for the reagents [6]. In this sense, ultrasound and microwave-based procedures have been suggested [2, 7].

Aiming to explore greener alternatives, miniaturisation strategies have been developed to significantly reduce the acid and sample amounts [6]. Moreover, this advantage can be interesting for samples, mainly clinical samples, which are usually available in small quantities. Micro-scaled procedures have been described in the context of closed-vessel microwave-assisted decomposition. In this sense, miniaturised vials were explored early on for the decomposition of several biological samples [8, 9]. Early polypropylene (PP) vials with 2 mL of capacity were explored for the decomposition of human hair, aiming to determine As and Se by HGAAS [10, 11]. Brancalion et al. [8] proposed a customised system for Cd determination in plants by thermospray flame furnace atomic absorption spectrometry (TS-FF-AAS) that involves using four mini-vials inserted inside a microwave vessel.

From another perspective, the sample preparation field has received attention due to the need to find sustainable and safe reagents. Therefore, improving instruments, such as with higher pressure and temperature approaches, has made systems more efficient and less time-consuming. In addition, it is possible to explore new reagents due to these operational conditions (high pressure and temperature). In this sense, only in a pressurised system has hydrogen peroxide been reported for organic matrices, e.g. margarine, honey, cocoa butter, and olive oil. Recently, Muller et al. [12] proposed a method for the wet digestion of milk powder, which used a microwave containing a single reaction chamber operated at 200 bars for analysis by ICP-MS and ICP OES. A large sample (around 1 g) and 8 mL of H_2O_2 (50% v v⁻¹) were obtained as optimal conditions, and the residual carbon content (RCC) assessed was 918 mg L⁻¹.

It is important to highlight that another advantage of H_2O_2 is related to minimising non-spectral interferences which are usually caused by nitric acid, such as signal suppression, in ICP OES and ICP-MS. Fundamental studies have demonstrated the influence of nitric acid in argon plasma, such as on the ionisation processes and the reduction of plasma temperature (also called cooling effects) due to the energy required to break N–O bonds [13]. Considering that it is well known that water is the major product of H_2O_2 decomposition, these problems involving non-spectra interferences are

thus overcome [14]. The benefit of reducing the amount of acid is related to the blank signal, which is substantially minimised, hence improving the sensitivity. Moreover, there is less impact on the instrument's lifetime due to acid damage in some components, such as the cone, skimmer, and sample introduction system (nebuliser and spray chamber) [15]. In this context, this work aims to develop a new and greener methodology based on wet microwave-assisted digestion involving a miniaturised system and only hydrogen peroxide to decompose biological samples, e.g. urine from patients with COVID, serum, and plant in vitro biotechnological material (soy callus). The residual carbon content (RCC) was checked after each decomposition and the green metric approach was calculated for the proposed method according to AGREEprep software. Also, it is important to highlight that, to the best of our knowledge, it is the first time that these two green analytical chemistry strategies (miniaturisation and use of only hydrogen peroxide) have been employed in sample preparation for elemental analysis.

Material and methods

Instrumentation

The samples were decomposed in a microwave system (DGT-100 microwave oven, Provecto Analitica, Jundiaí, Brazil) composed of a magnetron (2450 ± 13 MHz). The developed approach for microdecomposition involves using a holder with four positions to insert micro-vials composed of polytetrafluoroethylene (PTFE) with the same dimensions of Cryovial® polypropylene (PP) mini-vials of 2 mL. This system is inserted inside a microwave flask containing 10 mL of water. It is important to highlight that all of these components are composed of PTFE. A design of the system used is shown in Fig. 1.

An ICP-MS (iCAP TQ, Thermo Scientific, Bremen, Germany) and an ICP OES (iCAP 6300 Duo Series ICP OES, Thermo Fisher Scientific, Bremen, Germany) were employed to perform the measurements. The emission lines monitored were as follows: 396.8 nm (Ca); 279.5 (Mg); 257.6 nm (Mn); 213.6 nm (P), and 182 nm (S). The ICP-MS was tuned daily with a solution composed of Bi, Li, Co, Ce, In, and U ($1 \mu\text{g L}^{-1}$) and a 99.999% pure argon dewar was used to supply the ICP-MS (White Martins-Praxair, São Paulo, Brazil). The equipment was operated with 1550 W of RF power, 5 mm of sampling depth, 14 L min⁻¹ of cool flow, 0.99 mL min⁻¹ of nebuliser flow, and a sample introduction system composed of a concentric nebuliser (Micromist model) and a cyclonic spray chamber. The ICP OES parameters employed were 1350 W of plasma power, 0.80 L min⁻¹ of nebuliser gas flow, and 0.5 L min⁻¹ of auxiliary gas flow, while a concentric nebuliser and cyclonic spray chamber

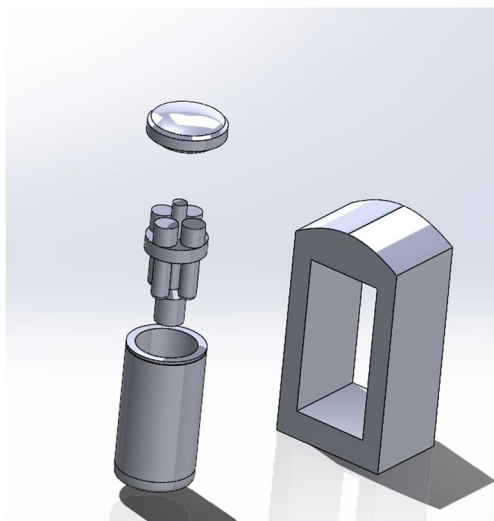


Fig. 1 Design of miniaturised system used for microwave-based decomposition procedure

Table 1 Operational conditions used for inductively coupled plasma optical emission spectrometry (ICP OES)

Parameter	
RF power	1150 W
Analysis pump rate	5 rpm
Nebuliser gas flow	0.7 L min ⁻¹
Auxiliary gas flow	0.5 L min ⁻¹
Plasma viewing	Axial (S, Mn, and P) and radial (Mg and Ca)
Emission lines	396.8 nm (Ca); 279.5 (Mg); 257.6 nm (Mn); 213.6 nm (P); and 182 nm (S)
Nebuliser	Concentric
Spray chamber	Cyclonic

were used as the introduction system. Moreover, the reaction and collision cell (CRC) was pressurised with helium and operated in the kinetic energy discrimination, oxygen, and ammonium to reduce the spectral interferences. He-KED was used for ⁵⁶Fe, ⁶⁴Zn, ⁵⁸Ni, ⁵⁹Co, and ¹¹¹Cd. The analysis of ⁸⁰Se was performed in the mass-shift mode ($m/z = 96$) and using oxygen as reaction gas. Finally, the ammonium was used for ⁵⁷Fe determination in serum samples. The analysis of possible subproducts formed during the decomposition was carried out by LTQ-Orbitrap Thermo Fisher Scientific mass spectrometry system (Bremen, Germany) and the data were analysed with Xcalibur software (Thermo Scientific). The information about the instrument's operational condition is listed in Tables 1, 2, and 3 for ICP OES, ICP-MS, and LTQ-Orbitrap, respectively.

Samples, solutions, and reagents

The standards and samples were prepared using deionised water (≥ 18.2 M Ω cm) acquired from a Milli-Q water purification system (Millipore, Bedford, USA). The hydrogen peroxide used was purchased from Merck (Darmstadt, Germany). The nitric acid (Merck, Darmstadt, Germany) employed for sample preparation and to adjust the acidity of samples and calibration solutions was twice sub-boiled. The calibration solutions were prepared using mono-elemental standards (Fluka, Buchs, Switzerland). Regarding calibration solutions used in ICP-MS, the linear range applied for determination of Cd, Co, Mn, Mo, Ni, and Se was from 0.05 to 10 $\mu\text{g L}^{-1}$, and for Cu, Zn, and Fe, it ranged from 0.5 to 100 $\mu\text{g L}^{-1}$. For analysis in ICP OES, the linear ranges used were as follows: 0.2–20 mg L⁻¹ for Ca; 0.1–10 mg L⁻¹ for P, S, and Mg; and 0.01–1 mg L⁻¹ for Mn.

Table 2 Operational conditions used for inductively coupled plasma mass spectrometry (ICP-MS)

Parameters	
RF power	1550 W
Sampling depth	5 mm
Plasma gas flow	14 L min ⁻¹
Nebuliser gas flow	0.99 L min ⁻¹
Auxiliary gas flow	0.8 L min ⁻¹
Interface	High sensitivity insert
Spray chamber and nebuliser	Quartz cyclonic spray chamber (cooled at 2.7 °C); borosilicate glass micro-mist concentric nebuliser pumped at 50 rpm
He gas flow (KED)	4.3 mL min ⁻¹
O ₂ gas flow	0.3 mL min ⁻¹
NH ₃ gas flow	0.3 mL min ⁻¹
Isotopes	⁵⁶ Fe (urine sample), ⁵⁷ Fe (serum sample), ⁶⁴ Zn, ⁵⁸ Ni, ⁵⁹ Co, ¹¹¹ Cd, ⁸⁰ Se, ⁹⁸ Mo

Table 3 Operational conditions used for Q-Exactive Quadrupole Orbitrap mass spectrometer

Parameter	
Spray voltage (+)	3500 V
Spray voltage (-)	3200 V
Spray current	1.8 μ A
Capillary temperature	300 °C
Sheath gas	35
Auxiliary gas	10
Spare gas	0
Max spray current (+)	100
Max spray current (-)	100
Ion source	HESI
Probe heater temperature	300
Acquisition mode	Full scan
Full scan resolution	70000
Scan range (m/z)	50–750

For the carbon curve used to assess RCC, citric acid (Merck) was diluted, and the calibration range employed was from 1 to 500 mg L⁻¹. The accuracy was assessed using certified reference materials of serum (ClinChek® Serum Control, lyophil., for trace elements, Level II) and urine (ClinChek® Urine Control, lyophil., for trace elements, Level II), both purchased from Recipe (München, Germany). Urine samples ($n = 10$) were collected from patients diagnosed with COVID-19 in partnership with a project approved by the Research Ethics Committee of the Federal University of Juiz de Fora (UFJF) together with the State University of Campinas (UNICAMP), registered under protocol number 4.566.092. Samples were refrigerated between 2 and 8 °C until analysis.

A Murashige and Skoog medium (Sigma-Aldrich, St. Louis, MO, USA) was used for soybean callus production. First, for callus induction, the medium was supplemented with sucrose (Synth, São Paulo, Brazil), agar (Merck, Darmstadt, Germany), casein hydrolysate (Sigma-Aldrich, St. Louis, MO, USA), and 2,4-dichlorophenoxyacetic acid (Sigma-Aldrich, St. Louis, MO, USA). Finally, during callus propagation, thiamine (Sigma-Aldrich, St. Louis, MO, USA) and myo-inositol (Sigma-Aldrich, St. Louis, MO, USA) were employed. The detailed procedure can be found in the literature [16].

Sample preparation

The proposed method based on microwave-assisted wet digestion involves only hydrogen peroxide. To this end, 100 μ L of urine or serum was decomposed using 300 μ L of H₂O₂ (30% v v⁻¹). For soybean in vitro material (callus), 50 mg was digested with 500 μ L of H₂O₂. The heating programme

comprised 5 min at 400 W, 20 min at 790 W, and 3 min at 320 W. Acid decomposition was performed to obtain results comparable to the proposed method for soybean callus samples due to the absence of certified reference material for this matrix. Therefore, 50 mg of soybean callus and 100 μ L of urine or serum were digested using 200 μ L of HNO₃ (14 mol L⁻¹) and 50 μ L of H₂O₂ (30% v v⁻¹). The microwave heating programme was the same as previously described in this section. After decomposition, the volumes were adjusted to 3–5 mL with deionised water.

Statistical analysis

The determination of the difference between the two groups was analysed using Student's *t*-test where $p < 0.05$ was considered significant. A boxplot was plotted with the average values of the variables and processed in GraphPad Prism® software.

Results

Establishment of decomposition parameters and evaluation of decomposition efficiency and accuracy

Human biological samples: urine and serum samples

For a preliminary result, the volume of urine and serum samples to be tested was evaluated for both 100 and 200 μ L. In visually analysing the digested product, the highest volume of sample (200 μ L) presented visible particulates, mainly in the serum samples. Therefore, the use of 100 μ L of sample was selected for future studies. First, the RCC was assessed to evaluate the proposed decomposition method, and the RCCs for urine and serum were determined to be 0.06% \pm 0.002 and 0.81% \pm 0.2, respectively. Although RCC was observed in these samples, the low values indicate the efficiency of the proposed decomposition method. Moreover, according to the literature, this amount of RCC has not induced non-spectral interferences caused by carbon, such as analyte signal enhancement or suppression due to a charge transfer mechanism, collisional ionisation, or collisional excitation with carbon-based species [17–19].

The method's accuracy was checked by comparing the observed values with certified values. For the urine sample (Table 4), the recovery was estimated from 82% (Ni) to 122% (Zn). These results indicate that the proposed method is suitable for this sample. For serum samples (Table 5), the proposed method is also suitable for determining Fe, Cu, Zn, Co, Se, Mo, Cd, and Mg; the recoveries found ranged from 72 to 105 when employing certified reference material. Moreover, as many elements (e.g. Fe, Cu, Zn, Mn, Ni, Co,

Table 4 Elemental concentration determined in certified reference material of urine by ICP OES (Mg and Ca) and ICP-MS (Cd, Co, Cu, Fe, Mn, Mo, Ni, Se, and Zn)

Analyte	Certified value ($\mu\text{g L}^{-1}$)	Found value ($\mu\text{g L}^{-1}$)	Trueness (%)
Ca	16.8	14.3 \pm 1.1	85
Cd	14.1	12.8 \pm 0.9	91
Co	9.5	8.9 \pm 1.5	94
Cu	104.0	102.0 \pm 8.9	98
Fe	222.0	250.0 \pm 58.6	91
Mg	45.1	45.4 \pm 1.5	101
Mn	9.5	8.5 \pm 0.5	90
Mo	93.0	96.5 \pm 3.5	104
Ni	14.6	12.0 \pm 0.1	82
Se	75.3	64.8 \pm 1.2	86
Zn	502	609.0 \pm 13.5	122

Table 5 Elemental concentration determined in certified serum reference material by ICP OES (Mg) and ICP-MS (Cd, Co, Cu, Fe, Mo, Se, and Zn)

Analyte	Certified value ($\mu\text{g L}^{-1}$)	Found value ($\mu\text{g L}^{-1}$)	Trueness (%)
Cd	5.9	4.2 \pm 0.3	72
Co	5.7	4.70 \pm 0.2	82
Cu	1400	1238.0 \pm 59.2	88
Fe	1500	1357 \pm 126	91
Mg	21.8	19.5 \pm 0.1	105
Mo	5.8	4.7 \pm 0.1	81
Se	105	92.6 \pm 7.2	88
Zn	1700	1648 \pm 134	97

Se, Mo, Cd, Ca, and Mg) could be determined with good accuracy and precision, this method can be employed for diverse applications, such as clinical toxicological studies (Ni and Cd determination), metallomics studies involving the ionic profile due to the occurrence of a disease, and the relationship between trace elements and health disorders [20, 21].

The detection (LOD) and quantification (LOQ) limits were assessed according to IUPAC recommendations: three and ten times the blank standard deviation, respectively, divided by the slope obtained from the calibration curve. The values obtained from this method are presented in Table 6. The lowest detection limit found was for Cd ($0.001 \mu\text{g L}^{-1}$), while the highest was for Ca ($60 \mu\text{g L}^{-1}$).

Soybean callus

The amount of sample and the volume of hydrogen peroxide were initially investigated to determine the best

Table 6 Detection limit values estimated for the proposed method (serum and urine) using only hydrogen peroxide in a miniaturised system and ICP OES (Mg and Ca) and ICP-MS (Cd, Co, Cu, Fe, Mn, Mo, Ni, Se, and Zn) as detection techniques

Analyte	LOD ($\mu\text{g L}^{-1}$)	LOQ ($\mu\text{g L}^{-1}$)
Mn	0.10	0.34
Fe	0.50	1.67
Ni	0.02	0.06
Co	0.01	0.03
Cu	0.02	0.07
Zn	0.52	1.74
Se	0.002	0.007
Mo	0.01	0.02
Cd	0.001	0.002
Ca	60.00	240.00
Mg	10.00	20.00

decomposition conditions. Three sample amounts were tested in this context: 10, 25, and 50 mg and two H_2O_2 volumes: 300 and 500 μL . In these preliminary results, 500 μL was more suitable, in terms of decomposition efficiency; therefore, the experiments were carried on with this condition. In the supplementary material, in Section 1, there are some descriptions about the development and optimisation of the digestion method based on the use of only hydrogen peroxide.

The decomposition efficiency was assessed by analysing residual carbon by ICP OES. The RCC was below the detection limit for all conditions, indicating that the proposed method was efficient for plant *in vitro* biotechnological materials. On the other hand, seven elements (Zn, Mo, Ca, Mg, Mn, P, and S) were determined by ICP-MS and ICP OES, aiming to compare with the proposed method (Table 7). Based on the results, the values found in the digestion method employing only hydrogen peroxide are compared to the established decomposition method for biological matrices, which usually uses nitric acid combined with H_2O_2 [2] and satisfactory values were observed for the three sample masses tested. Regarding the sampling precision, there is a trend for the mass range used (10–50 mg); the low masses, 10 mg and 20 mg, show the highest relative standard deviation (RSD), mainly for Ca and Zn. Therefore, considering this extremely heterogeneous matrix, a high mass is recommended to avoid bias and poor repeatability. In addition, increasing the sample amount results in sensitivity and precision enhancements. In this context, the best condition defined for this sample was 50 mg of soybean callus and 500 μL of H_2O_2 (30% $v v^{-1}$).

The detection limit was assessed according to recommendation of IUPAC, and for both methods (acid and hydrogen

Table 7 Elemental concentration ($\mu\text{g g}^{-1}$) determined in soybean callus samples employing the proposed digestion method (only hydrogen peroxide) and its comparison with the acid-based digestion. For

both decomposition procedures, ICP OES (Ca, Mg, P, S, and Mn) and ICP-MS (Mo and Zn) were used as detection techniques

Analyte ($\mu\text{g g}^{-1}$)	Acid decomposition		Hydrogen peroxide decomposition					
	50 mg		50 mg	Agreement (%) ^a	20 mg	Agreement (%) ^a	10 mg	Agreement (%) ^a
Ca	258.3 ± 13.7		260.2 ± 16.7	101	263.0 ± 42.8	102	268.6 ± 44.3	111
Mg	60.9 ± 1.4		65.7 ± 3.1	108	68.1 ± 1.4	112	59.0 ± 3.8	97
Mn	8.1 ± 0.7		8.7 ± 0.5	107	8.4 ± 0.4	104	8.8 ± 0.7	109
Mo	0.31 ± 0.05		0.27 ± 0.01	87	0.27 ± 0.01	87	0.26 ± 0.05	84
P	112.0 ± 3.9		132.6 ± 6.5	118	127.1 ± 9.6	113	113.1 ± 15.0	101
S	162.0 ± 6.5		186.9 ± 12.1	115	179.6 ± 8.5	111	164.7 ± 8.1	102
Zn	3.8 ± 0.6		3.1 ± 0.2	82	3.6 ± 1.2	95	5.3 ± 3.3	139

^aValues obtained by comparing the values found in the proposed method and nitric acid decomposition**Table 8** Detection limit values obtained for acid and hydrogen peroxide decomposition of soybean callus samples using ICP OES (Ca, Mg, P, S, and Mn) and ICP-MS (Mo and Zn) as detection techniques

Limit of detection	Acid decomposition	Hydrogen peroxide decomposition
Ca ($\mu\text{g g}^{-1}$)	2.1	9.1
Mg ($\mu\text{g g}^{-1}$)	1.2	2.8
Mn (ng g^{-1})	43.9	13.0
Mo (ng g^{-1})	4.0	3.0
P ($\mu\text{g g}^{-1}$)	9.4	5.9
S ($\mu\text{g g}^{-1}$)	14.4	13.7
Zn (ng g^{-1})	1.2	1.1

peroxide decomposition), it is shown in Table 8. According to the results, the decomposition procedure with only hydrogen peroxide had LOD values lower than the acid composition for Mn, Mo, and P.

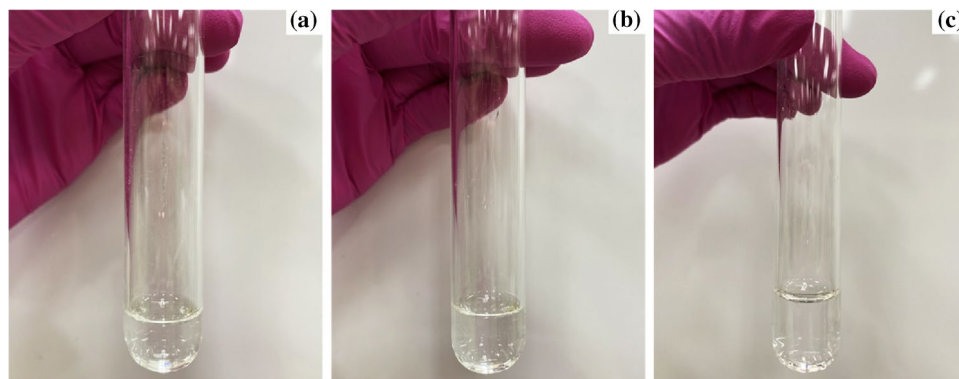
Considerations for the sample preparation process

Hydrogen peroxide is characterised as a weak acid and as a substance with oxidising properties. Moreover, this

reagent has been considered “green” due to the products of decomposition, which are only water and oxygen [12, 14]. In this context, the use of H_2O_2 has great promise for the principles of green chemistry in addition to the instrumental advantages discussed previously. The final aspect of digested samples (soybean callus, urine, and serum) is shown in Fig. 2.

Further experiments are performed to clarify some insights, such as the possible products formed. First, an experiment was performed to check the acidity of the digested material. Ten replicates containing 500 μL of H_2O_2 were run in the heating microwave programme; afterward, they were mixed, and pH was recorded. The initial pH was 2.82 ± 0.05 , and the final value was 1.27 ± 0.15 , indicating the formation of acid species and an enhanced factor of 36 related to hydronium formation during microwave-assisted decomposition. This result is relevant because it corroborates the importance of acid species formation, which can contribute to the decomposition of the sample. The same observation was reported by Muller et al. [12] during the decomposition of milk powder with only hydrogen peroxide in a high-pressure system. The pH initially recorded was 4, while the final pH was 3. Moreover, another study investigating the microwave radiation effect in water

Fig. 2 The final aspect of the samples digested with only hydrogen peroxide, in a miniaturised system, and after adjusting the final volume. **a** Soybean callus; **b** urine; **c** serum



observed that increasing microwave exposure time reduces pH [22].

A solution containing only H_2O_2 (30% v v⁻¹) was submitted to microwave-assisted digestion with the same heating program previously described to evaluate which products can be formed during decomposition. After this process, the solution was directly injected into the LTQ-Orbitrap, and the analysis was run in negative mode. A peak derived from nitrate (NO_3^-) was found at $m/z = 61.99$ (Fig. 3), thus indicating the formation of nitric acid in situ. This nitric acid production is probably related to NO_x recombination and water vapor [22]. Moreover, the high temperature and pressure in the miniaturised vials contribute to these processes [23]. The acid formation corroborates the pH decreases that were discussed above. Figueiredo et al. reported the presence of nitrate and other anions (e.g. fluoride, chloride, and sulfate) in water after microwave heating. Furthermore, an increase in microwave radiation exposure increases the amount of NO_3^- . According to the authors, some compounds in the air, such as nitrogen, contribute to these anions in the digested sample [22].

Green analytical chemistry metrics

Aiming to assess the procedure's greenness, a recently released software called AGREEprep (Analytical greenness metric for sample preparation) was employed [24]. The main

advantage of this approach is that it considers all principles of GAC flexibly combined with green sample preparation (GSP), some of which have not been considered in other available software. Overall, the software scores the analytical procedure from 0 to 1, with a higher value corresponding to a more desirable GSP condition. The 10 principles of GSP are presented in this approach, among them miniaturisation, sample amount, energy consumption, sample throughput, waste production, and operator safety. Moreover, the weight for each principle used was in the default condition as recommended.

In this sense, the H_2O_2 decomposition procedure was compared with three different acid-based methods described in the literature [25–27]. It is important to highlight that the energy consumption was estimated employing the same microwave system used in this work; therefore, the difference of value was due to the several powers and times employed in the heating program. The pictogram with the metrics is shown in Fig. 4, and more details about the methods described in the literature are discussed in the supplementary material (Table S2).

According to the results, the H_2O_2 decomposition showed a score value of 0.42 for callus decomposition and 0.45 for urine and serum decomposition. Moreover, the green metric for the miniaturised method employed nitric acid and hydrogen peroxide described for callus samples showed a value of 0.42. Comparing both miniaturised methods (hydrogen peroxide and acid decomposition), it is possible to see that

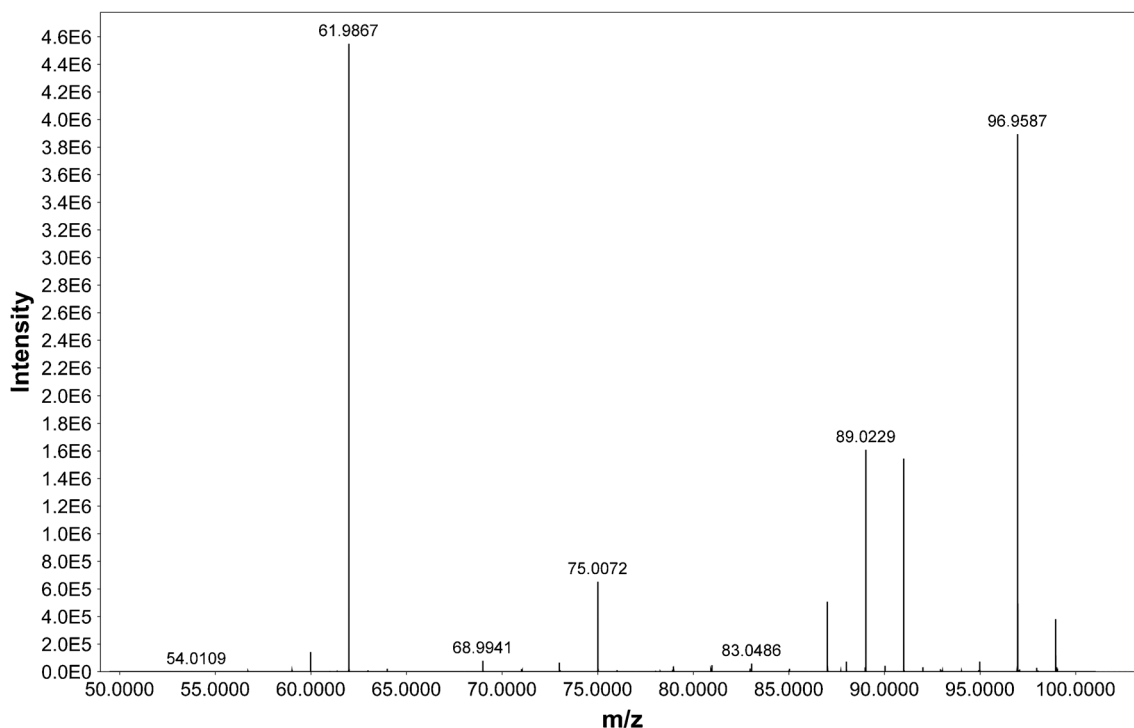


Fig. 3 The mass spectrum of a solution composed of hydrogen peroxide after decomposition

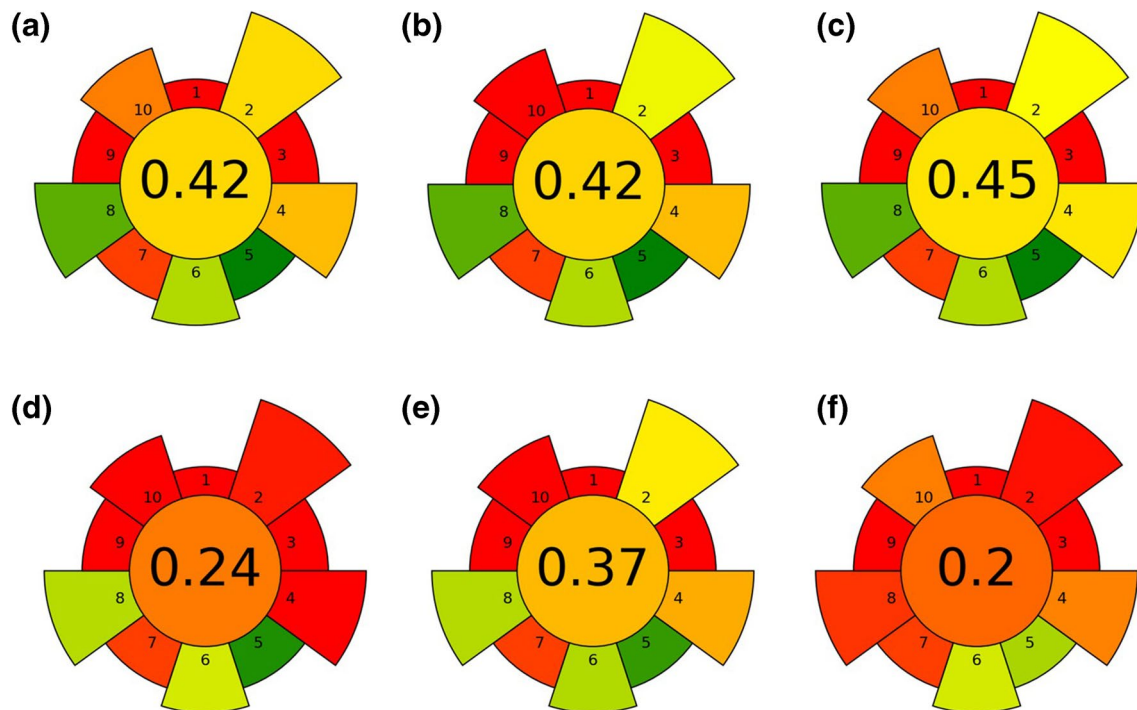


Fig. 4 AGREEprep scores were obtained for the conventional (a) H_2O_2 microdecomposition for callus samples (our work); b HNO_3 microdecomposition for callus samples (our work); c H_2O_2 microdecomposition for urine and serum samples (our work); d Arruda et al.

— callus (acid decomposition) [25]; e Grassin-Delyle et al. — biological samples (acid decomposition) [26]; f Zhang et al. — urine samples (acid decomposition) [27]

criterion 10 (Ensure safe procedures for the operator) is significantly affected by using nitric acid and H_2O_2 , which has more than four safety pictograms. Moreover, three conventional closed-vessel microwave decompositions for callus samples and urine showed critical metric values, around 0.2 - 0.37. This observation is related to the high amount of sample and reagents used, which affects Criterion 2 and 5; hence, the waste generated tends to increase in this conventional procedure (Criterion 4). Furthermore, the sample throughput is diminished (Criterion 6) due to the capability of running 16 samples in a batch with miniaturised decomposition, as opposed to the conventional method which allows for only 12 samples per batch.

Applications

Urinary metal concentrations in patients with COVID-19

The analytical methodology was applied to 20 urine samples (10 COVID-19 positive and 10 control) to determine Mn, Fe, Ni, Co, Cu, Zn, Se, Mo, Cd, Ca, and Mg content by ICP-MS and ICP OES. The results in Fig. 5 indicate statistical differences in the Ca, Cd, Co, and Mg ($p < \alpha$) levels between urine samples from patients with COVID-19 and control samples. However, levels of all elements except Cu (with an

average concentration of $4.7 \mu\text{g L}^{-1}$) were higher in COVID-19 samples than in controls, suggesting increased excretion.

During COVID-19 viral infection, studies show that metals play important roles in the complex interactions between the virus and cells in the human body. This is because most metals are present in the form of metalloproteins that are involved as agents in the immune response and the deregulation of the system [28]. The elements calcium and magnesium, for example, were associated with severe and post-mortem stages in patients with COVID-19 in a study carried out by Guerrero-Romero et al. [29]. However, there is still a gap to understanding the homeostasis of these metals in individuals with COVID-19. Some results have indicated Fe, Zn, and Cu as targets for studies on biochemical pathways during viral disease [30].

In this context, Aryal et al. analysed plasma samples from healthy patients and patients with COVID-19. To digest the samples, the authors used an oven at 80°C for 4 h in concentrated HNO_3 , repeating the procedure twice for a total of 8 h. As a main result, they found that the concentration of copper increased significantly in plasma samples with COVID-19 compared to control samples [31].

Zeng et al. [32] conducted a study of 138 patients with COVID-19 to assess urinary concentrations of chromium, manganese, copper, selenium, cadmium, mercury, and lead

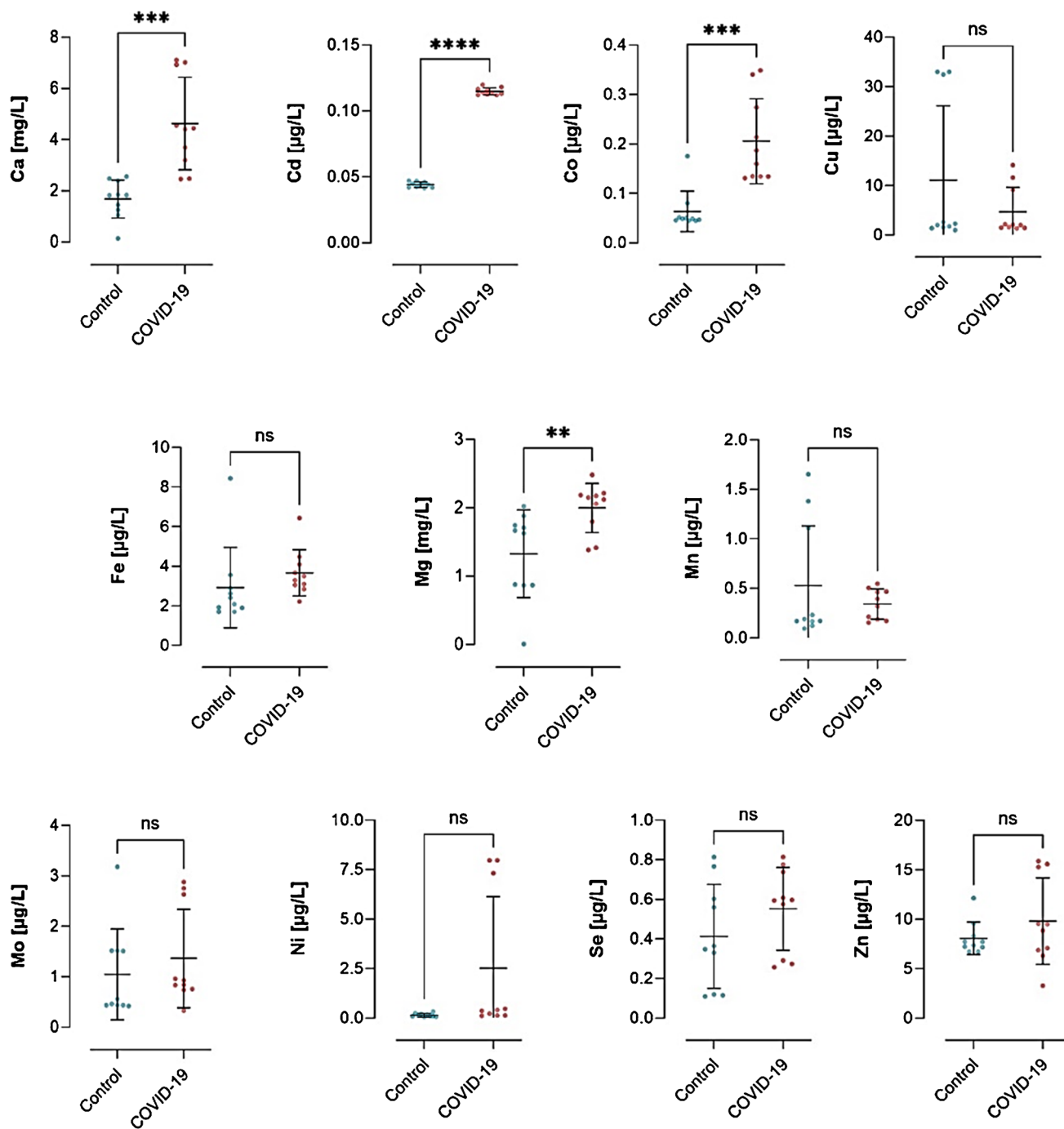


Fig. 5 Average concentrations of metals in urine from control patients and those diagnosed with COVID-19. Error bars show mean values \pm standard deviation. p values were calculated using the non-

paired t -test. Statistical significance is indicated as ns not significant ($p > 0.05$), $*p \leq 0.05$ and $**p \leq 0.01$, $***p \leq 0.001$ and $****p \leq 0.0001$

from the onset of the disease and over its clinical course. For sample preparation, 400 μ L of urine was diluted in a solution of Triton X-100 and HNO_3 . This sample preparation strategy is critical and may affect the accuracy of the results due to the non-ionic surfactant effect of Triton X-100, which leads

to a decrease in the amount of metal available for ionisation in the plasma [33]. The results pointed to abnormalities in the urinary levels of trace metals, mainly the element Cu, and associated high levels of Cu with severe states of the disease and fatal outcomes of COVID-19 [32].

Table 9 Determination of micro- and macronutrients in soybean callus samples employing the proposed sample preparation method and ICP OES (Ca, Mg, P, S, and Mn) and ICP-MS (Mo and Zn) as detection techniques

Sample	Ca ($\mu\text{g g}^{-1}$)	Mg ($\mu\text{g g}^{-1}$)	Mn ($\mu\text{g g}^{-1}$)	Mo (ng g^{-1})	P ($\mu\text{g g}^{-1}$)	S ($\mu\text{g g}^{-1}$)	Zn (ng g^{-1})
60 nm	390.2 \pm 22.0	77.1 \pm 4.5	8.8 \pm 0.4	289.4 \pm 19.5	52.8 \pm 6.5	131.3 \pm 7.1	5494.5 \pm 315.7
Control	304.6 \pm 11.9	58.2 \pm 8.7	6.8 \pm 0.9	200.8 \pm 31.7	30.8 \pm 5.4	83.9 \pm 8.5	4018.2 \pm 799.3
Control	385.1 \pm 55.6	76.2 \pm 9.7	9.2 \pm 1.2	207.7 \pm 23.1	49.6 \pm 5.5	119.1 \pm 13.9	4467.1 \pm 491.1
Control	426.1 \pm 59.5	81.5 \pm 12.1	9.8 \pm 1.3	175.2 \pm 2.1	52.9 \pm 5.7	124.0 \pm 14.0	4214.8 \pm 54.1
Control	305.5 \pm 40.0	61.5 \pm 7.1	7.6 \pm 0.8	224.9 \pm 18.1	42.9 \pm 3.8	107.4 \pm 5.7	5110.4 \pm 18.11

Excessive levels of iron and zinc may be related to the activity of the virus in the system, which increases mutation rates and requires greater activity of the immune response [34]. In this sense, Alkattan et al. [35] studied the association between Zn, Fe, Cu, and Se in the blood during viral infection by COVID-19. The authors detected different levels of elements in blood plasma, such as zinc concentrations in the range of 120 mcg/dL, iron 776 mcg/dL, and copper 18 mcg/dL, respectively. In this work, excessive levels of iron and zinc were also detected in urine samples from patients with COVID-19 disease.

In summary, the analytical method developed in this work is suitable for clinical studies and toxicological tests, in addition to helping to define the factors associated with the severity of COVID-19 and predicting clinical outcomes to improve the prognosis of the disease. It has the advantages of using a low volume of sample and reagent, having a shorter preparation time, and being environmentally friendly, in addition to ensuring the accuracy of the results obtained.

Determination of micro- and macronutrients in soybean callus cultivated in the presence of silver nanoparticles

Plant tissue culture, also called PTC, has been highlighted in the biotechnology field due to several possibilities, such as genetic, pharmaceutical, cosmetic, and bioenergetic research. One of the most interesting products of this *in vitro* process is the plant callus, which is composed of pre-existing stem cells. This material is produced from any plant part (*e.g.* stem, leaf, root, or seed) in an aseptic medium under controlled conditions (temperature and photoperiod) [36, 37]. Moreover, the culture of plant suspension cells is produced from callus employing a culture medium under shaking, and this process is widely used for studies at the single-cell level [38]. Recently, nanotechnology has been combined with the plant *in vitro* cultures, and opportunities have been highlighted such as the production of secondary metabolites [39, 40]. From another perspective, the *in vitro* plant cultures can also be used for toxicological investigations [41]. Considering the importance of biotechnological material, the analysis of trace elements provides relevant information, for example,

in the determination of elements involved in biochemical pathways or the internalisation of a target analyte.

In this context, the proposed method is an important tool for these studies. For evaluation of the applicability of the sample preparation procedure, five samples of soybean callus were cultivated in the presence of silver nanoparticles with a nominal size of 60 nm and at a concentration of 400 $\mu\text{g L}^{-1}$. Samples collected from the medium without silver nanoparticles were analysed and named “control”. The results for the determination of seven elements (Ca, Mg, Mn, Mo, S, P, and Zn) are shown in Table 9. According to the results, the elements with the highest concentrations were Ca, S, and Mg, with values ranging 305–426 mg g^{-1} , 84–131 mg g^{-1} , and 58–82 mg g^{-1} , respectively. Conversely, Mo was the element with the lowest concentration (175–289 $\mu\text{g g}^{-1}$). Moreover, comparing the soybean callus cultivated in the presence of silver nanoparticles with the soybean callus control, there were no verified differences among the elemental concentrations. Kučerová et al. [42] employed an analytical method for the determination of nutrients in poplar calli cultivated in the presence of arsenic and silicon based on acid digestion (4 mL of concentrated HNO_3 and 2 mL of H_2O_2), flame atomic absorption spectrometry (FAAS), and ICP-MS. The nutrient concentrations that they observe agree with those found in this work, and Ca is the element present in the highest amounts.

Conclusion

According to the results, the proposed method is an excellent alternative for sample preparation of biological samples in the context of green chemistry, mainly for procedures with applications for disease monitoring and biotechnology. The miniaturised method significantly reduced the quantity of both samples and reagents, thus contributing to the greenness of the method. Additionally, using only hydrogen peroxide as a reagent greatly impacts other analytical issues, such as by improving sensibility due to a cleaner blank and reducing non-spectral interferences in plasma-based techniques which are caused by nitric acid. Concerning the analytical parameters, the

method's accuracy was satisfactory for all matrices, showing trueness above 72% for all the analytes investigated. Moreover, the assessment of RCC (less than 0.8%) in the samples after decomposition indicates the efficiency of the method.

Supplementary Information The online version contains supplementary material available at <https://doi.org/10.1007/s00216-024-05472-w>.

Author contribution Ana Beatriz Santos da Silva: writing — original draft, validation, methodology, formal analysis, data curation, conceptualisation. software, formal analysis, data curation. Ketolly Natanne da Silva Leal: writing — original draft, validation, methodology, formal analysis, data curation, conceptualisation. software, formal analysis, data curation. Marco Aurélio Zezzi Arruda: writing — review and editing, writing — original draft, visualisation, supervision, project administration, funding acquisition, conceptualisation.

Funding This work was financially supported by Fundação de Amparo à Pesquisa do Estado de São Paulo (FAPESP 2014/50867–3, 2018/25207–0, 2019/24445–8, 2020/06934–9, and 2020/08543–7), and Conselho Nacional de Desenvolvimento Científico e Tecnológico—CNPq grant number 303231/2020–3, and the scholarship SWE-CNPq 200475/2022–3. Furthermore, the authors would like to thank Professor Marcone Augusto Leal Oliveira for providing the urine samples.

Declarations

Ethics approval Urine samples were acquired after authorisation by the Ethics Committee from the University Hospital of the Federal University of Juiz de Fora (Acceptance codes: 4.473.404; 4.566.092; 5.039.371) and the Ethics Committee from the Federal University of Juiz de Fora (Acceptance code 5.267.924). The target individuals were people above 18 years old that formally agreed to participate by signing the Free and Informed Consent Form and the anamnesis questionnaire.

Conflict of interest The authors declare no competing interests.

References

- Santana APR, Nascimento PA, Guimarães TGS, Ribeiro Menezes IMNR, Andrade DF, Oliveira A, et al. (Re) thinking towards a sustainable analytical chemistry: Part I: Inorganic elemental sample treatment, and Part II: Alternative solvents and extraction techniques. *TrAC Trends Anal Chem.* 2022;152:116596. <https://doi.org/10.1016/j.trac.2022.116596>.
- Bizzi CA, Pedrotti MF, Silva JS, Barin JS, Nóbrega JA, Flores EMM. Microwave-assisted digestion methods: Towards greener approaches for plasma-based analytical techniques. *J Anal At Spectrom.* 2017;32:1448–66. <https://doi.org/10.1039/c7ja00108h>.
- Wrobel K, Kannamkumarath S, Wrobel K, Caruso JA. Environmentally friendly sample treatment for speciation analysis by hyphenated techniques. *Green Chem.* 2003;5:250–9. <https://doi.org/10.1039/b208213f>.
- López-Lorente ÁI, Pena-Pereira F, Pedersen-Bjergaard S, Zuin VG, Ozkan SA, Psillakis E. The ten principles of green sample preparation. *TrAC Trends Anal Chem.* 2022;148:116530. <https://doi.org/10.1016/j.trac.2022.116530>.
- Nowak PM. What does it mean that “something is green”? The fundamentals of a Unified Greenness Theory. *Green Chem.* 2023;25:4625–40. <https://doi.org/10.1039/d3gc00800b>.
- Gonzalez MH, Souza GB, Oliveira RV, Forato LA, Nóbrega JA, Nogueira ARA. Microwave-assisted digestion procedures for biological samples with diluted nitric acid: Identification of reaction products. *Talanta.* 2009;79:396–401. <https://doi.org/10.1016/j.talanta.2009.04.001>.
- Jesus JR, Arruda MAZ. A feasible strategy based on high ultrasound frequency and mass spectrometry for discriminating individuals diagnosed with bipolar disorder and schizophrenia through ionic profile. *Rapid Commun Mass Spectrom.* 2020;34:1–10. <https://doi.org/10.1002/rcm.8798>.
- Brancalion ML, Arruda MAZ. Evaluation of medicinal plant decomposition efficiency using microwave ovens and mini-vials for Cd determination by TS-FF-AAS. *Microchim Acta.* 2005;150:283–90. <https://doi.org/10.1007/s00604-005-0357-0>.
- Costa LF, Tormena CF, Arruda MAZ. Ionics and lipidomics for evaluating the transgenic (cp4-EPSPS gene) and non-transgenic soybean seed generations. *Microchem J.* 2021;165:0–2. <https://doi.org/10.1016/j.microc.2021.106130>.
- Flores EMM, Saidelles APF, Barin JS, Mortari SR, Martins AF. Hair sample decomposition using polypropylene vials for determination of arsenic by hydride generation atomic absorption spectrometry. *J Anal At Spectrom.* 2001;16:1419–23. <https://doi.org/10.1039/b107910g>.
- Mortari SR, Saidelles APF, Barin JS, Flores EMM, Martins AF. A simple procedure for decomposition of human hair using polypropylene vials for selenium determination by hydride generation atomic absorption spectrometry. *Microchim Acta.* 2004;148:157–62. <https://doi.org/10.1007/s00604-004-0250-2>.
- Muller EI, Souza JP, Muller CC, Muller ALH, Mello PA, Bizzi CA. Microwave-assisted wet digestion with H₂O₂ at high temperature and pressure using single reaction chamber for elemental determination in milk powder by ICP-OES and ICP-MS. *Talanta.* 2016;156:232–8. <https://doi.org/10.1016/j.talanta.2016.05.019>.
- Grotti M, Todolí JL. Nitric acid effect in inductively coupled plasma mass spectrometry: New insights on possible causes and correction. *J Anal At Spectrom.* 2020;35:1959–68. <https://doi.org/10.1039/d0ja00130a>.
- Ciriminna R, Albanese L, Meneguzzo F, Pagliaro M. Hydrogen peroxide: A key chemical for today's sustainable development. *ChemSusChem.* 2016;9:3374–81. <https://doi.org/10.1002/cssc.201600895>.
- de Oliveira AF, da Silva CS, Bianchi SR, Nogueira ARA. The use of diluted formic acid in sample preparation for macro- and micro-elements determination in foodstuff samples using ICP OES. *J Food Compos Anal.* 2018;66:7–12. <https://doi.org/10.1016/j.jfca.2017.11.001>.
- da Silva ABS, Arruda MAZ. Exploring single-particle ICP-MS as an important tool for the characterization and quantification of silver nanoparticles in a soybean cell culture. *Spectrochim Acta Part B At Spectrosc.* 2023;203:106663. <https://doi.org/10.1016/j.sab.2023.106663>.
- Serrano R, Grindlay G, Gras L, Mora J. Insight into the origin of carbon matrix effects on the emission signal of atomic lines in inductively coupled plasma optical emission spectrometry. *Spectrochim Acta Part B At Spectrosc.* 2021;177:106070. <https://doi.org/10.1016/J.SAB.2021.106070>.
- Grindlay G, Gras L, Mora J, De Loos-Vollebregt MTC. Carbon-, sulfur-, and phosphorus-based charge transfer reactions in inductively coupled plasma-atomic emission spectrometry. *Spectrochim Acta Part B At Spectrosc.* 2016;115:8–15. <https://doi.org/10.1016/J.SAB.2015.10.010>.
- Wiltsche H, Winkler M, Tirk P. Matrix effects of carbon and bromine in inductively coupled plasma optical emission spectrometry. *J Anal At Spectrom.* 2015;30:2223–34. <https://doi.org/10.1039/c5ja00237k>.

20. Arruda MAZ, de Jesus JR, Blindauer CA, Stewart AJ. Specimics as a concept involving chemical speciation and omics. *J Proteomics*. 2022;263:104615. <https://doi.org/10.1016/j.jprot.2022.104615>.
21. Subashchandrabose S, Pereira-Filho ER, Donati GL. Trace element analysis of urine by ICP-MS/MS to identify urinary tract infection. *J Anal At Spectrom*. 2017;32:1590–4. <https://doi.org/10.1039/c7ja00141j>.
22. Figueiredo EC, Dias JC, Kubota LT, Korn M, Oliveira PV, Arruda MAZ. Influence of microwave heating on fluoride, chloride, nitrate and sulfate concentrations in water. *Talanta*. 2011;85:2707–10. <https://doi.org/10.1016/j.talanta.2011.08.003>.
23. Bizzi CA, Flores EMM, Barin JS, Garcia EE, Nóbrega JA. Understanding the process of microwave-assisted digestion combining diluted nitric acid and oxygen as auxiliary reagent. *Microchem J*. 2011;99:193–6. <https://doi.org/10.1016/j.microc.2011.05.002>.
24. Wojnowski W, Tobiszewski M, Pena-Pereira F, Psillakis E. AGREeprep – Analytical greenness metric for sample preparation. *TrAC Trends Anal Chem*. 2022;149:116553. <https://doi.org/10.1016/j.trac.2022.116553>.
25. Arruda SCC, Rodríguez APM, Arruda MAZ. Ultrasound-assisted extraction of Ca, K and Mg from in vitro citrus culture. *J Braz Chem Soc*. 2003;14:470–4. <https://doi.org/10.1590/S0103-50532003000300023>.
26. Grassin-Delyle S, Martin M, Hamzaoui O, Lamy E, Jayle C, Sage E, Etting I, Devillier P, Alvarez JC. A high-resolution ICP-MS method for the determination of 38 inorganic elements in human whole blood, urine, hair and tissues after microwave digestion. *Talanta*. 2019;199:228–37. <https://doi.org/10.1016/j.talanta.2019.02.068>.
27. Zhang T, Chang X, Liu W, Li X, Wang F, Huang L, Liao S, Liu X, Zhang Y, Zhao Y. Comparison of sodium, potassium, calcium, magnesium, zinc, copper and iron concentrations of elements in 24-h urine and spot urine in hypertensive patients with healthy renal function. *J Trace Elem Med Biol*. 2017;44:104–8. <https://doi.org/10.1016/j.jtemb.2017.06.006>.
28. De Jesus JR, de Andrade TA. Understanding the relationship between viral infections and trace elements from a metallomics perspective: Implications for COVID-19. *Metallomics*. 2020;12:1912–30. <https://doi.org/10.1039/d0mt00220h>.
29. Guerrero-Romero F, Mercado M, Rodríguez-Moran M, Ramírez-Rentería C, Martínez-Aguilar G, Marrero-Rodríguez D, Ferreira-Hermosillo A, Simental-Mendía LE, Remba-Shapiro I, Gamboa-Gómez CI, Albarrán-Sánchez A, Sanchez-García ML. Magnesium-to-calcium ratio and mortality from COVID-19. *Nutrients*. 2022;14:1686. <https://doi.org/10.3390/nu14091686>.
30. De Jesus JR, Galazzi RM, Lopes Júnior CA, Arruda MAZ. Trace element homeostasis in the neurological system after SARS-CoV-2 infection: Insight into potential biochemical mechanisms. *J Trace Elem Med Biol*. 2022;71:126964. <https://doi.org/10.1016/j.jtemb.2022.126964>.
31. Aryal B, Tillotson J, Ok K, Stoltzfus AT, Michel SLJ, Rao VA. Metal-induced oxidative stress and human plasma protein oxidation after SARS-CoV-2 infection. *Sci Rep*. 2023;13:2441. <https://doi.org/10.1038/s41598-023-29119-5>.
32. Zeng H-L, Zhang B, Wang X, Yang Q, Cheng L. Urinary trace elements in association with disease severity and outcome in patients with COVID-19. *Environ Res*. 2021;194:110670. <https://doi.org/10.1016/j.envres.2020.110670>.
33. Lisboa MT, Clasen CD, de Vellar DCS, Oreste EQ, Saint'Pierre TD, Ribeiro AS, Vieira MA. An Easy and Fast Procedure for the Determination of Ca, Cu, Fe, Mn, Mg, Na, K and Si in Biodiesel by ICP OES Using Emulsification as Sample Preparation Strategy. *J Braz Chem Soc*. 2013;25:143–51. <https://doi.org/10.5935/0103-5053.20130280>.
34. Anuk AT, Polat N, Akdas S, Erol SA, Tanacan A, Biriken D, Keskin HL, Moraloglu Tekin O, Yazihan N, Sahin D. The Relation Between Trace Element Status (Zinc, Copper, Magnesium) and Clinical Outcomes in COVID-19 Infection During Pregnancy. *Biol Trace Elem Res*. 2021;199:3608–17. <https://doi.org/10.1007/s12011-020-02496-y>.
35. Alkattan A, Alabdulkareem K, Kamel A, Abdelseed H, Almutairi Y, Alsalamene E. Correlation between Micronutrient plasma concentration and disease severity in COVID-19 patients. *Alexandria J Med*. 2021;57(1):21–7. <https://doi.org/10.1080/20905068.2020.1870788>.
36. Thorpe TA. History of plant tissue culture. In: Loyola-Vargas V, Ochoa-Alejo N, editors. *Plant cell culture protocols*. Methods Mol Biol. 2007;37:169–80. https://doi.org/10.1007/978-1-61779-818-4_2.
37. Chun SC, Gopal J, Iyyakannu S, Muthu M. An analytical retrospection of mass spectrometric tools established for plant tissue culture: Current endeavours and future perspectives. *TrAC Trends Anal Chem*. 2020;126:115843. <https://doi.org/10.1016/j.trac.2020.115843>.
38. Mustafa NR, De Winter W, Van Iren F, Verpoorte R. Initiation, growth and cryopreservation of plant cell suspension cultures. *Nat Protoc*. 2011;6:715–42. <https://doi.org/10.1038/nprot.2010.144>.
39. Jayasankar D, Jayasankar V, Subramanian J. NanoAOX—a novel nanoparticle and antioxidant mixture enhances the growth of plants in vitro and in vivo. *Vitr Cell Dev Biol Plant*. 2022;58:407–15. <https://doi.org/10.1007/s11627-021-10242-9>.
40. Dumani Y, Mortazavian SMM, Izadi-Darbandi A, Ramshini H, Amini F. Titanium dioxide nanoparticles affect somatic embryo initiation, development, and biochemical composition in *Paulownia* sp. seedlings. *Ind Crops Prod*. 2022;176:114398. <https://doi.org/10.1016/j.indcrop.2021.114398>.
41. Arruda MAZ, da Silva ABS, Kato LS. There is plenty of room in plant science: nanobiotechnology as an emerging area applied to somatic embryogenesis. *J Agric Food Chem*. 2023;71:3651–7. <https://doi.org/10.1021/acs.jafc.2c08065>.
42. Kučerová D, Vivodová Z, Kollárová K. Silicon alleviates the negative effects of arsenic in poplar callus in relation to its nutrient concentrations. *Plant Cell Tissue Organ Cult*. 2021;145:275–89. <https://doi.org/10.1007/s11240-020-02007-w>.

Publisher's Note Springer Nature remains neutral with regard to jurisdictional claims in published maps and institutional affiliations.

Springer Nature or its licensor (e.g. a society or other partner) holds exclusive rights to this article under a publishing agreement with the author(s) or other rightsholder(s); author self-archiving of the accepted manuscript version of this article is solely governed by the terms of such publishing agreement and applicable law.